中国科学: 技术科学 2023 年 第 53 卷 第 8 期: 1255 ~ 1271
SCIENTIA SINICA Technologica techcn.scichina.com
《中国科学》杂志社 SCIENCE CHINA PRESS

评 述 庆祝国防科技大学建校70周年机械工程学科专辑

高精度微机电陀螺研究现状与发展趋势

席翔, 孙江坤, 肖定邦*, 张勇猛, 李青松, 周鑫, 卢坤, 石岩, 侯占强, 吴学忠*

国防科技大学智能科学学院, 长沙 410073
* E-mail: dingbangxiao@nudt.edu.cn; xzwu@nudt.edu.cn

收稿日期: 2023-03-22; 接受日期: 2023-06-06; 网络版发表日期: 2023-07-28
国家自然科学基金面上项目(批准号: 52075540)和国家自然科学基金重点项目(批准号: 51935013)资助

摘要 微机电陀螺具有体积功耗小、重量轻、成本低等优势, 在工业与国防装备中广泛应用. 高精度的微机电陀螺可提升多类装备、平台姿态测控精度, 有望解决无人车、无人机等装备在复杂环境下的自主导航问题, 发展前景广阔, 因而始终是惯性领域的热点研究方向之一. 但是高精度微机电陀螺研制面临的技术挑战同样十分巨大, 本文首先梳理了高精度微机电陀螺的结构演变规律, 并将其分为质量块式结构以及旋转对称式结构进行了性能分析与对比. 接着针对微机电陀螺表头品质提升问题, 总结了微谐振结构的品质因数提升方法以及频率修调方法, 然后按照速率模式、速率积分模式以及频率调制模式介绍了高精度微机电陀螺控制技术研究现状. 最后, 本文对高精度微机电陀螺的发展和应用趋势进行了展望.

关键词 高精度微机电陀螺, 谐振结构, 零偏不稳定性, 品质因数, 频率裂解, 控制技术

1 引言

陀螺是测量物体旋转运动角速度和角度的传感器, 是多类装备实现姿态测量、惯性导航和运动控制等功能的核心器件. 高精度的陀螺在国防和工业建设领域均具有重要的应用价值, 因此其始终是世界科技强国重点发展的核心器件之一. 传统上, 高精度的陀螺类型主要有机械陀螺、光学陀螺(激光陀螺、光纤陀螺)和半球谐振陀螺等. 它们虽然能够达到较高的性能, 但是也存在体积和重量大、功耗高、部件多、加工成本高等缺点, 制约了其应用范围. 20世纪90年代以后, 微机电系统技术进步和微制造水平不断提升, 推动低成本、小体积的微机电陀螺发展, 并快速占领消费电子、车辆安全等中低端市场份额[1]. 但是, 小体积重量却也制约了微机电陀螺性能的提升, 诸如结构灵敏度相对较低、热机械噪声大、易受环境扰动等问题长期难以解决, 使其在高端工业设备和武器装备中的应用面临很大考验[2~4].

因此, 高精度微机电陀螺是目前惯性领域最具吸引力的研究方向之一. 一旦微机电陀螺突破当前精度瓶颈进入导航级, 将使绝大部分惯性导航系统具备性能、体积、成本和功耗的综合优势, 对工业、电子设备、国防装备以及航空航天等领域带来变革性的影响(图1). 但与此同时, 高端微机电陀螺的研制也是业内公认的最具挑战性的课题. 一方面微制造工艺较之传统制造工艺相对加工误差大, 微尺寸误差、微观缺陷等影响

引用格式: 席翔, 孙江坤, 肖定邦, 等. 高精度微机电陀螺研究现状与发展趋势. 中国科学: 技术科学, 2023, 53: 1255–1271
Xi X, Sun J K, Xiao D B, et al. Research status and development trend of high-precision MEMS gyroscope (in Chinese). Sci Sin Tech, 2023, 53: 1255–1271, doi: 10.1360/SST-2023-0119

© 2023 《中国科学》杂志社

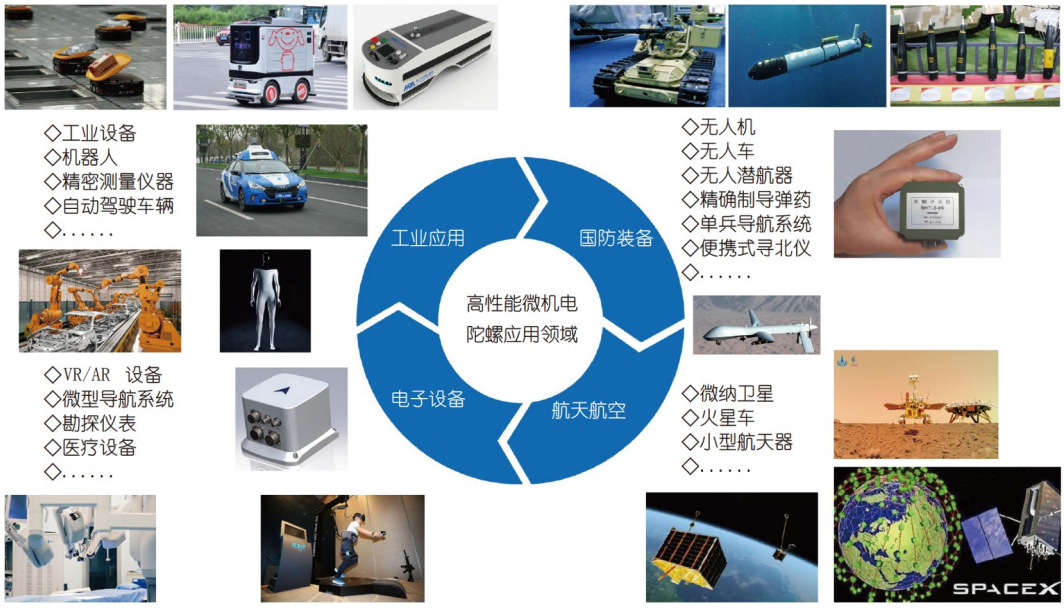


图 1 微机电陀螺应用场景
Figure 1 Application scenario of MEMS gyroscope.

效应突显, 致使陀螺核心结构的品质很难满足高精度微机电陀螺的需求. 另外一方面微机电陀螺因结构尺寸小, 对自身耦合振动以及温度、应力等扰动更为敏感, 需要高精度、多参数的控制以及大量误差补偿, 对误差理论建模以及测控电路提出了更高的要求.

但是总体而言, 近10年微机电陀螺性能提升的趋势十分明显, 受益于新的结构形式、工艺方法以及测控技术进步, 已报道有多个微机电陀螺处于导航级精度门槛. 同时新的控制模式使微机电陀螺的误差自标定、自补偿能力得到很大提升, 面对外部环境展示出更加优异的性能, 体现出智能化的端倪. 本文通过回顾近些年较高精度的微机电陀螺技术发展, 重点梳理了其结构演变规律、品质提升方法, 以及其前沿控制技术的研究现状, 并对行业发展趋势进行了展望, 旨在为本领域相关技术研究提供参考.

2 高精度微机电陀螺谐振结构演变

2.1 质量块式微机电陀螺

2.1.1 单质量块微机电陀螺

从微机电陀螺的质量-弹簧基本动力学模型出发, 其大致可分为集中质量块式结构与分布式质量结构. 其中单质量块式结构由弹性结构支撑振动质量块, 是基本动力学模型的最直观体现[5~7]. 其通常设计为解耦结构形式, 例如典型的万向节微振动结构, 一个质量块被两个可以扭转的嵌套外框架所支撑[8,9]. 如图2所示, 陀螺工作时, 中心质量块以一定的振幅和频率沿着固定方向扭转振动; 当有角速度输入时, 将在另一个方向因哥氏力也发生振动, 振动幅值与角速度输入呈正比.

可以通过调节结构参数增大振动位移的方式提升单质量块陀螺灵敏度, 如Alper等人[10]利用梳齿式驱动结构增加了单质量块振动陀螺的驱动力; Leoncini等人[11]设计了折叠梁结构增加陀螺的振动位移. 但是单质量块结构因非中心对称的振型, 品质因数和抗冲击

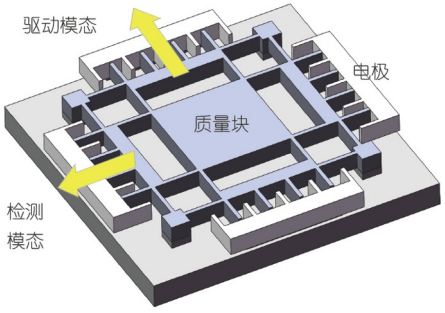


图 2 典型的单质量块微机电陀螺结构[10]
Figure 2 Typical structure of a single mass MEMS gyroscope [10].

性能受到限制, 少有高精度性能报道.

2.1.2　双质量块微机电陀螺

在单质量块式结构的基础上, 将谐振结构设计为两个振型对称的质量块, 则形成双质量块微机电陀螺(又名音叉式陀螺), 典型结构如图3所示[12]. 这种设计可以解决结构振动时带来的质心偏摆问题, 有效降低支撑损耗, 使微机电陀螺具备中高精度潜力[13~21]. Honeywell公司最新报道的音叉式微机电陀螺零偏不稳定性(以下均指Allan方差)为0.02°/h, 量程大于990°/s, 标度因数非线性为13 ppm. 法国Tronics公司开发的梳齿式电极结构陀螺零偏不稳定性为0.8°/h, 量程为±300°/s, 标度因数非线性为230 ppm[22].

我国东南大学提出了一种双质量块解耦音叉式陀螺, 在温控环境下样机零偏不稳定性为0.2°/h, 量程为±100°/s, 标度因数非线性为60 ppm[23~26]. 南京理工大学采用圆片级封装工艺制备的音叉式陀螺零偏不稳定性为0.18°/h, 量程为±300°/s, 标度因数非线性为136.6 ppm[27,28]. 西安飞行自动控制研究所也报道了零偏稳定性优于0.66°/h的音叉式微机电陀螺[29].

2.1.3　四质量块微机电陀螺

为了进一步增加质量块分布的对称性, 在双质量块微机电陀螺的基础上又进一步演化出四质量块微机电陀螺[30~31], 其一般由四个对称分布的质量块通过梁结构连接而成, 惯性质量和品质因数得到进一步提高, 因此具有较好的灵敏度和机械热噪声水平.

四质量块微机电陀螺因结构对称性可工作在频率匹配模式以提高检测灵敏度. 加州大学欧文分校Asadian等人[32]设计了基于反相对称工作模态的四质量块微机电陀螺, 工作时支点处于力平衡状态, 因而支撑损耗十分小. 同时, 通过减小谐振频率和壁厚达到降低结构热弹性阻尼的效果, 品质因数可接近2×10^6. 速率积分模式下该陀螺的零偏不稳定性为0.2°/h, 角度随机游走为0.02°/$h^{1/2}$, 量程可以超过1000°/s[33]. 在力反馈模式下, 其角度随机游走为0.015°/$h^{1/2}$, 零偏不稳定性为0.09°/h[34]. 清华大学设计了采用十字梁支撑的四质量块微机电陀螺(图4), 相邻质量块之间通过折弯柔性梁相互连接, 工作检测模态均呈现对称状, Q值为16000[35,36]. 零偏不稳定性为0.12°/h, 角度随机游走为0.012°/$h^{1/2}$[37].

四质量块微机电陀螺也可以工作在非对称的驱动检测模态, 同样体现出较好的性能. Sensonor公司在IMEGO研究所四质量块谐振结构的基础上研制了蝶翼式微机电陀螺, 结构如图5(a)所示[38]. 其最新STIM300系列产品量程为±400°/s, 常温下零偏不稳定性为0.5°/h, 具有较好的零偏温度敏感度(0.08°/h/°C)以及标度因数非线性(15 ppm)[39]. 国防科技大学对蝶翼式硅微陀螺的敏感结构进行了优化设计, 结构如图5(b)所示, 采用全预掩埋工艺有效减小了加工误差, 实现硅斜梁的精确加工. 同时通过应力释放与平衡结构有效减小了陀螺加工中的热应力结构变形和封装应力, 零偏不稳定性为0.19°/h, 量程为±200°/s, 标度因数非线性为89.6 ppm[40~47].

2.2　旋转对称式微机电陀螺

2.2.1　二维环形微机电陀螺

将集中式的质量块结构沿圆周方向进行离散分

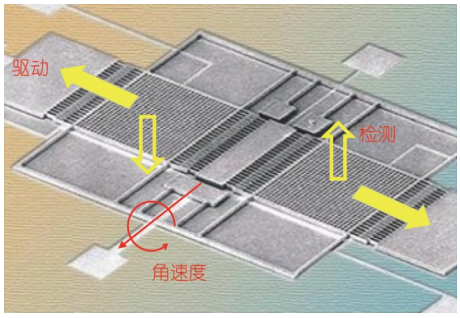


图 3　典型的高精度双质量块微机电陀螺结构[12]

Figure 3　Typical high-precision dual-mass MEMS gyroscope structure [12].

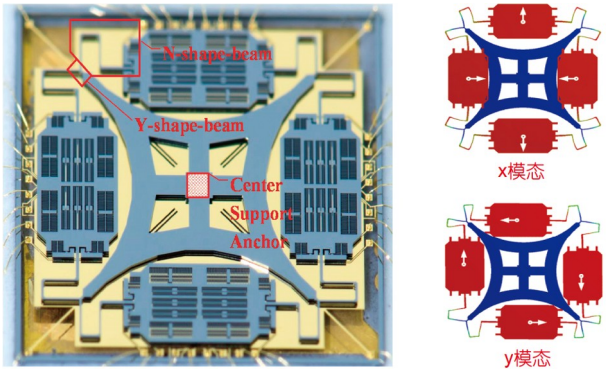


图 4　典型四质量块微机电陀螺结构及工作模态[37]

Figure 4　Structure and operating modes of the typical four-mass MEMS gyroscope [37].

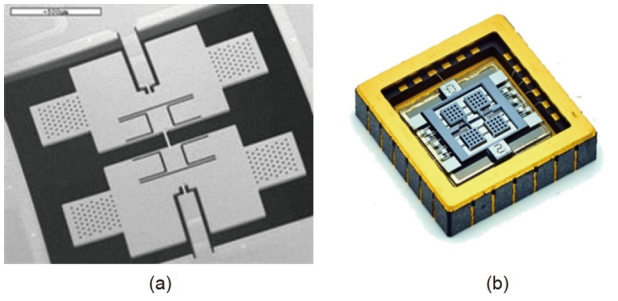


图 5 蝶翼式微机电陀螺结构. (a) Sensonor结构[38]; (b) 国防科技大学提出的结构

Figure 5 Structures of butterfly MEMS gyroscopes. (a) Structure proposed by Sensonor [38]; (b) structure proposed by National University of Defense Technology.

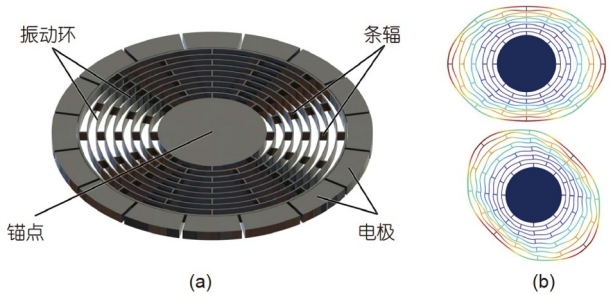


图 6 高精度环形微机电陀螺典型结构和工作模态. (a) 典型结构; (b) 工作模态

Figure 6 Typical structure and operating principle of the high-precision ring type MEMS gyroscope. (a) Typical structure; (b) operating modes.

布, 则形成旋转对称式结构的微机电陀螺. 其在几何上呈旋转轴对称状, 一般工作在匹配的模态, Q值高, 从而具有更好的精度潜力. 20世纪90年代起, 密歇根大学开始对较简单的单环式微机电陀螺的理论建模、材料以及工艺开展研究[48~51], 为环形微机电陀螺的发展奠定了基础. 目前环形微机电陀螺中应用较广泛的产品是Silicon Sensing公司的电磁环式陀螺, 其CRH02系列产品零偏不稳定性为0.12°/h, 量程为±400°/s, 利用电磁激励Z形梁支撑的硅环振动, 具有较好的抗冲击振动性能[52], 最新的CRH03系列产品零偏不稳定性达到0.03°/h, 但量程相对较小.

但是单个谐振环的有效振动质量较小, 仍存在机械热噪声较大的问题, 为提升环形微机电陀螺性能潜力, Boeing公司和喷气推进实验室(JPL)共同提出了由多个环嵌套而成的盘形微机电陀螺方案[53], 如图6所示, 直径约为8 mm, 各同心环通过辐射状横梁相连接, 不同环可以通过内部电极进行驱动、检测或刚度调节. 这种盘形结构具有更大的等效质量和驱动检测电容面积, 陀螺检测灵敏度和信噪比得到有效提升, 同时可通过结构优化设计将其机械热噪声降低至极低水平. 亚德诺半导体(AD)公司与斯坦福大学设计的盘形微机电陀螺频率匹配之后零偏不稳定性为0.2°/h[54,55], 但是具有较大的阻尼不匹配. 近年美国多所研究机构的盘形微机电陀螺研究进展迅速, 温控下样机零偏不稳定性最高可达到0.01°/h, 证实了导航级的精度潜力, 已达到寻北应用的要求[56].

盘形微机电陀螺因其多样化的结构参数而具有丰富的拓扑形态, 并展示出较好的性能潜力. 国防科技大学提出了基于刚度质量解耦原理的新型蜂巢式微机电陀螺, 其结构拓扑演化如图7所示. 通过质量刚度解耦设计方法使该陀螺品质因数达到650000, 零偏不稳定性达到0.018°/h, 角度随机游走为0.00684°/h$^{1/2}$. 苏州大学提出了16边形蛛网式微机电陀螺, 体现出较好的抗冲击特性.

2.2.2 三维微半球谐振陀螺

微半球陀螺由传统半球谐振陀螺演变而来, 也可认为是微机电陀螺由二维结构向三维结构的拓展, 其继承了半球谐振陀螺高品质因数的优良特性, 因而具备极高的精度潜力, 是当前高精度微机电陀螺最热点的研究方向之一. 近年来, 在美国国防部高级研究计划局(DARPA)的推动下, 加州大学、密歇根大学和佐治亚理工大学[57~65]、德雷珀(Draper)实验室[66,67]等多所研究机构开展了微半球陀螺探索, 主要结构形式包括半球形结构、盆形结构、酒杯状结构等.

高精度的微半球谐振结构目前主要由玻璃吹制法制造, 由密歇根大学最早提出. 其成形过程如图8所示, 在高温下熔融石英玻璃薄片产生非牛顿流体形变, 再通过真空吸气装置使薄片结构上下表面产生压力差, 实现直径5~10 mm的曲面壳体成形加工. 这种加工工

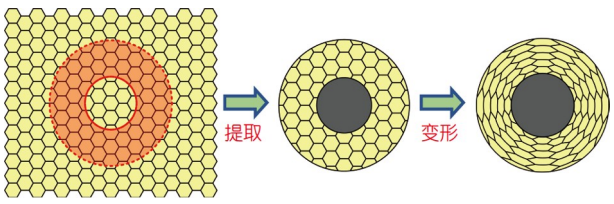


图 7 蜂巢式微机电陀螺结构拓扑演化

Figure 7 Structural topological evolution of the honeycomb MEMS gyroscope.

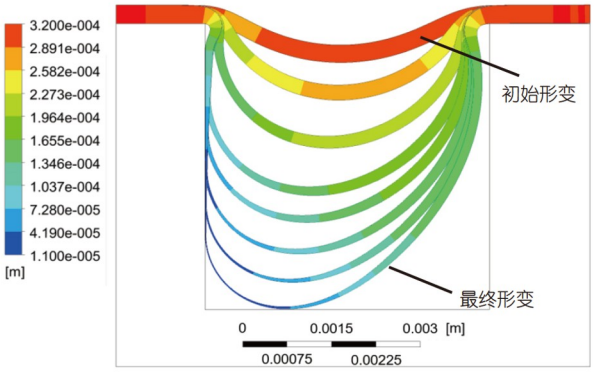


图 8　微半球谐振结构典型成形过程

Figure 8　Typical forming process of the micro hemispherical resonator.

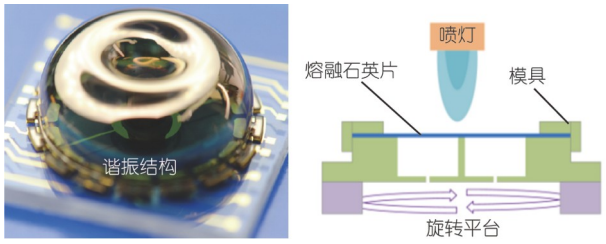


图 9　国防科技大学研制的微半球谐振陀螺结构与工艺

Figure 9　Structure and process of the micro-hemispherical resonant gyroscope proposed by National University of Defense Technology.

艺既具有较高效率，又避免了传统机械磨抛带来的亚表面损伤，表面粗糙度优于1 nm，未镀膜谐振结构品质因数最高可达9×10^6以上. 陀螺零偏不稳定性于2020年报道达到0.0014°/h, 显示出极大的精度潜力[68].

随着半球谐振陀螺研究的热潮，我国国防科技大学、清华大学、东南大学、上海交通大学、西北工业大学、南京理工大学、苏州大学、电子科技集团第26研究所等相关单位也开展了进一步研究. 东南大学研制的7 mm直径微半球谐振陀螺Q值为149200，在力平衡工作模式下，量程为±500°/s，零偏不稳定性为2.322°/h[69~72]. 国防科技大学为提高微半球谐振陀螺性能，提出了具有灵敏度放大结构的齿形微半球谐振结构，并开发了基于物理场调控的旋转吹制工艺与平台(图9)，有效提高了谐振结构的制造精度. 最高品质因数已超过4×10^6, 速率积分模式下陀螺零偏不稳定性为0.067°/h.

3　微机电陀螺谐振结构品质提升

3.1　品质因数提升

微机电陀螺的品质因数(Q值)主要受热弹性阻尼、支撑阻尼、空气阻尼等因素影响，提升方式主要有结构优化以及材料改进等. 斯坦福大学Kenny等人[79,80]发现影响盘形微机电陀螺Q值的关键因素之一为热弹性阻尼，并通过改变辐条尺寸来降低环与环之间的热传递(图10(a))，将结构Q值提升至180000. 国防科技大学通过多目标粒子群优化方法，建立了盘形微机电陀螺的嵌套环数量、尺寸参数与Q值之间的关系，并通过刚度质量解耦的结构设计方法大幅降低了热弹性阻尼带来的能量损耗，将Q值提升至510000，衰减时间常数为74.9 s[81~83]. 密歇根大学、国防科技大学建立了微半球谐振陀螺支撑阻尼损耗模型，如图10(b)所示，证实了不同支撑结构参数以及非理想几何误差对结构Q值具有重要影响[84].

在材料方面，寻求热弹性阻尼系数以及热膨胀系数更小的非硅基材料来替代传统硅基陀螺结构是当前热点方向之一. Boeing公司探索了基于熔融石英玻璃

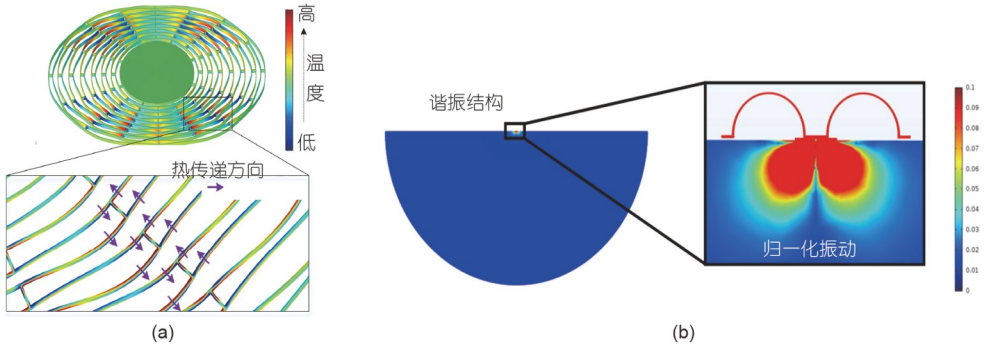


图 10　微机电陀螺品质因数影响机理. (a) 热弹性阻尼损耗影响; (b) 支撑阻尼损耗影响

Figure 10　Effect mechanism on quality factor of MEMS gyroscopes. (a) Thermoelastic damping loss effect; (b) support damping loss effect.

表 1 部分典型高精度微机电陀螺性能总结

Table 1 Performance summary of some typical high-precision MEMS gyroscopes

类型	研究单位	零偏不稳定性	量程	角度随机游走	标度因数非线性
双质量块微机电陀螺	Honeywell[22]	0.02°/h	>990°/s	0.0035°/h$^{1/2}$	13 ppm
	南京理工大学[73]	0.18°/h	±300°/s	–	136.6 ppm
	东南大学[24]	0.2°/h	±100°/s	–	60 ppm
四质量块微机电陀螺	加州大学欧文分校[34]	0.09°/h	–	0.015°/h$^{1/2}$	–
	国防科技大学[74]	0.19°/h	±200°/s	–	89.6 ppm
	清华大学[37]	0.12°/h	–	0.012°/h$^{1/2}$	–
二维环形微机电陀螺	Silicon Sensing[75]	0.03°/h	±10°/s	0.01°/h$^{1/2}$	–
	Boeing[56]	0.011°/h	–	0.003°/h$^{1/2}$	–
	加州大学[76]	0.11°/h	–	0.02°/h$^{1/2}$	–
	国防科技大学[77]	0.015°/h	±300°/s	0.00048°/h$^{1/2}$	–
三维微半球谐振陀螺	密歇根大学[68]	0.0014°/h	–	0.00016°/h$^{1/2}$	–
	国防科技大学[78]	0.067°/h	±7200°/s	–	0.79 ppm

的嵌套环陀螺, 期望将其品质因数提高到5×10^6[53]. 而熔融石英微半球谐振结构品质因数已经接近10^7. 但由此带来的非硅基制造工艺挑战也十分巨大, 目前在批量化以及一致性等方面尚不能做到与硅基工艺相当的水平.

还有些学者通过电路控制实现陀螺Q值提升, 如Nitzan等人[85]通过引入非线性刚度效应, 形成参数泵提升检测模态的Q值, 从而将陀螺的机械灵敏度提升67倍.

3.2 频率匹配性提升

微机电陀螺频率匹配是提高其检测灵敏度的关键, 方法主要有提高结构误差鲁棒性、机械修调和静电修调等. 对于硅基对称型微机电陀螺, 由于硅材料各向异性, 工作检测模态之间天然存在着较大频率裂解. 斯坦福大学研究者通过改变辐条结构位置和宽度参数, 使工作模态具有一致的质量刚度分布, 将(100)盘形微机电陀螺的初始频率裂解从大于10000 Hz减小至100 Hz以内[86,87]. 通过结构周期化拓扑也可以在一定程度上减小频率裂解, 如国防科技大学蜂巢式谐振结构、苏州大学蛛网式谐振结构, 均使硅片晶向误差导致的频率裂解得以改善[88].

但通过结构优化改善频率裂解适用范围较为有限, 因此利用静电负刚度效应调节模态频率是目前微机电陀螺中应用较多的修调方法[89]. 但难点在于频率裂解与正交误差相关, 而当陀螺闭环控制后正交误差会被抑制, 频率裂解缺乏观测量. 所以一般只能做开环修调, 频率匹配易受温度、应力、驱动电压等影响, 长期稳定性不够理想. 亚德诺半导体(AD)公司提出了一种基于振型扰动的闭环频率匹配技术, 并在盘形微机电陀螺上进行了验证, 实现了零偏稳定性0.2°/h的水平[54,55], 但缺点是工作带宽较小. 2022年法国赛峰公司基于其框架式微机电陀螺(图11(a)), 通过调节振动质量之间的机械耦合系数控制两种面内振动模态的频率差, 提升陀螺对于外界环境振动的鲁棒性. 图11(b)为该公司采用的质量动态平衡技术方案. 该方案在固定端引入附加质量m_0、附加弹簧k_0来测量质量不平衡误差, 并通过动态控制回路调节刚度k_1、k_2, 实现质量动态平衡[90]. 经过平衡后, 该陀螺室温下零偏不稳定性达到0.007°/h, 展示出优异的精度水平. 而且在

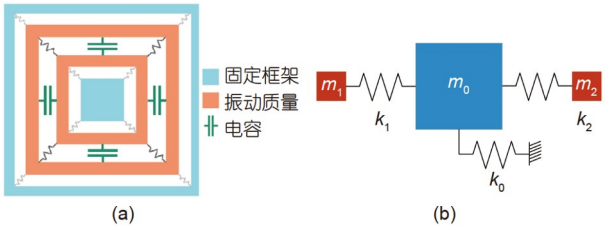


图 11 Safran公司提出的动态修调与平衡技术方案[91]. (a) 陀螺结构; (b) 质量平衡方案

Figure 11 Safran' dynamic adjustment and balance technical scheme proposed by Safran company [91]. (a) Structure of gyroscope; (b) method of mass balance.

−40°C~90°C的温度范围内零偏变化0.1°/h，在频带范围为10~2000 Hz (9g RMS)的振动环境下零偏变化0.3°/h[91].

但是无论结构优化或是静电修调均无法实现对结构本身固有缺陷的抑制，因此微机电陀螺的机械修调也受到充分关注. 频率裂解调节理论已相对成熟，关键难点在于如何精确辨识微结构的质量/刚度误差并实施调控，常规技术手段有在结构上添加质量(图12(a)), 或在一定区域内去除材料等方式. 加州大学洛杉矶分校Schwartz等人[92,93]通过在盘形微机电陀螺分布式焊点添加焊料的方法同时实现了n=2和n=3工作模态的修调，频率裂解分别降低至0.1 Hz和1.2 Hz. 2014年，密歇根大学利用微细超声加工设备，在熔融石英壳体上去除50 μm圆形范围内的材料，修调效率约为20 ng/min[94]. 2016年，Draper实验室通过飞秒激光刻蚀将多晶金刚石微半球谐振结构频率裂解从35.5 Hz降低到0.5 Hz以内[67]. Silicon Sensing公司也有通过激光修调环形硅微陀螺的报道. 2017年, 加州大学提出了研磨释放修调工艺，将谐振结构频率裂解从41 Hz减小至7 Hz[58]. 同年佐治亚理工大学提出了微半球谐振结构激光焊接修调工艺[95]. 国防科技大学研究了飞秒激光对熔融石英结构的微损伤机理，并在微半球谐振结构上实现了0.1 Hz以内的修调，修调孔形貌如图12(b)所示. 但总体而言，目前各种修调手段均存在一定局限性，0.1 Hz内的高精度、高效率机械修调仍面临较大挑战.

3.3　热应力控制

热应力导致的结构变形会使陀螺敏感结构的振型产生缓慢变化，是陀螺频率偏移和零偏漂移的直接原因[97,98]. 加州大学欧文分校对微机电陀螺封装应力进行了研究，显示其主要来源于材料特性的不匹配[99]. 纽约州立大学联合亚德诺半导体(AD)公司建立了热应力作用下陀螺的误差理论模型，提升了结构在应力作用下的鲁棒性，温度稳定性改善了5倍以上[100,101]. 韩国忠北大学提出了一种多折叠梁式的应力释放结构，将陀螺工作频率随温度的漂移减小了75%[102]. 日本研究人员设计了单边开口框架进行热应力隔离，使陀螺工作时驱动频率漂移仅2 Hz，零偏不稳定性达到0.9°/h[103]. 英国Silicon Sensing公司和美国佐治亚理工大学采用Z形弯曲梁支撑降低环形微机电陀螺的温度效应，在−40°C~125°C温度范围陀螺的标度因数变化降低了3倍[104~106].

对微机电陀螺实施温控也是改善温度应力的有效方法之一. 密歇根大学Najafi等人[107]提出了可以隔离热和振动的微机电陀螺封装，通过内部微加热器对微机电陀螺温度进行闭环控制，使微陀螺全温区频率温度稳定性(0.22 ppm/°C)和零偏不稳定性(0.55°/h)均得到明显改善[108]. 斯坦福大学Kenny等人提出了利用品质因数和工作频率差异等对振动结构进行温控的方案[109~111], 使微机电陀螺标度因数保持稳定.

4　高精度微机电陀螺控制技术

4.1　速率模式

由于速率模式下微机电陀螺的控制方式发展已久, 相关文献众多[112], 本节不再赘述, 重点对部分新进展进行介绍.

为了对速率工作模式下微机电陀螺的零偏漂移误差进行自补偿，Boeing公司提出了一种基于工作模态翻转的技术方案，如图13所示. 该方法将盘形微机电陀螺驱动、检测模态进行周期性的交换，由于在不同

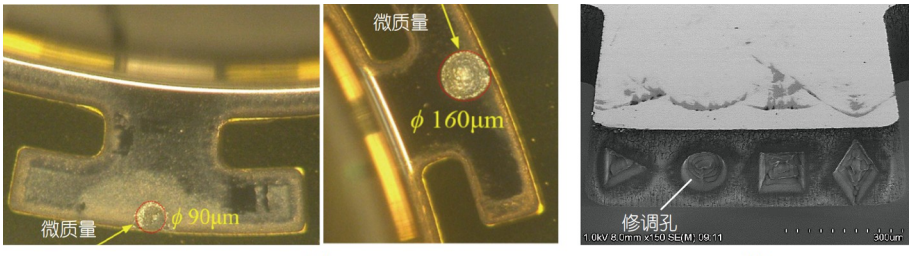


图 12　典型微机电陀螺机械修调方式. (a) 增加质量式修调; (b) 去除质量式修调[96]

Figure 12　Typical mechanical trimming methods of MEMS gyroscopes. (a) Adding mass trimming; (b) removing mass trimming [96].

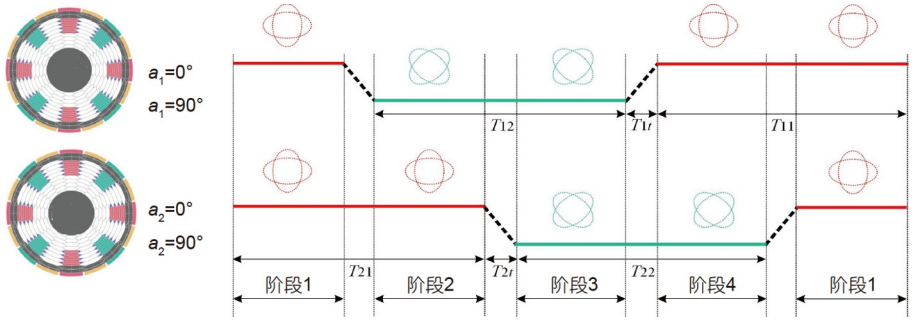


图 13 模态交换工作模式的时序配置
Figure 13 Timing configuration of modal exchange mode.

模态方位下阻尼不对称引发的陀螺漂移趋势正好相反, 因此该方法可实现对阻尼漂移的补偿, 使陀螺零偏不稳定性、零偏重复性均达到了0.01°/h[53]. 但由于谐振结构翻转模态需要不停起振, 单个陀螺的带宽很难保证, 因此可以采用多个陀螺的冗余配置保证始终有一个陀螺正常输出角速度[113]. 国防科技大学将模态翻转技术运用于蜂巢式微机电陀螺及其寻北仪样机, 陀螺零偏不稳定性达到0.0078°/h, 零偏重复性达到0.012°/h. 寻北仪室内寻北精度达到0.22°, 车载环境下寻北精度达到0.58°.

微机电陀螺一般采用静电电容驱动, 通常期望获得较大的振动幅值, 但当振动位移较大时将产生非线性现象, 一是机械结构本身的非线性响应, 二是静电驱动与检测中的非线性项变得不可忽略[114]. 两者均使结构动力学方程中的刚度系数出现了高阶项, 造成测控困难. 但也有不少学者开展了利用非线性效应提升陀螺性能的相关工作, 如加州大学戴维斯分校基于达芬方程使陀螺的振动处于非线性区间, 基本控制原理框图如图14所示, 最大振幅稳定达到陀螺间隙的3.8%, 有效提升了陀螺的零偏不稳定性和角速度随机游走[115].

4.2 速率积分模式

法国物理学家傅科1981年设计的傅科摆可以认为是速率积分陀螺的基本原型. 1995年美国人Lynch提出了“均值法”, 简化了谐振陀螺的理论模型, 该动力学模型含有刚度轴和阻尼误差项, 为速率积分陀螺的发展奠定了理论基础[116]. 因为速率积分模式对陀螺谐振结构对称性要求高, 最初只在半球谐振陀螺上实现较好效果. 近年来, 随着微机电陀螺谐振结构品质的提升,

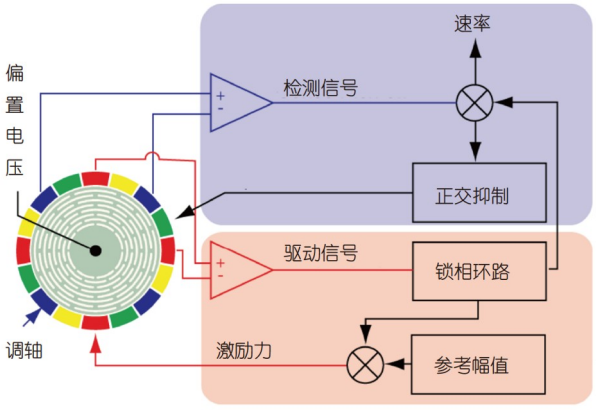


图 14 盘形微机电陀螺非线性闭环控制技术[115]
Figure 14 Nonlinear closed-loop control of the disk MEMS gyroscope [115].

速率积分型微机电陀螺开始迅速发展.

2012年加州大学欧文分校研究了速率积分模式的四质量块微机电陀螺, 角度输出的均方根非线性低于1%[117,118]. 加州大学戴维斯分校、欧文分校和伯克利分校先后实现了速率积分工作模式的盘形微机电陀螺[119,120]. 2014年密歇根大学研制的速率积分微半球谐振陀螺, 量程可达700°/s[121~123]. 2018年斯坦福大学利用振型自进动的方式将盘形微机电陀螺的速率阈值由40°/s降低至3°/s[124,125]. 我国清华大学实现了速率积分四质量块谐振陀螺的研制, 具有较大的角度增益(Ag=0.97)[35]. 南京理工大学初步研制了速率积分盘形微机电陀螺[126]. 国防科技大学通过非线性效应动态补偿、检测通道误差补偿、驱动通道误差补偿等方法, 使微半球谐振陀螺的零偏不稳定性达到0.067°/h, 量程大于7200°/s, 标度因数非线性达到0.78 ppm(图15). 在高速旋转大约689380°后陀螺仅有−0.56°的角度跟踪

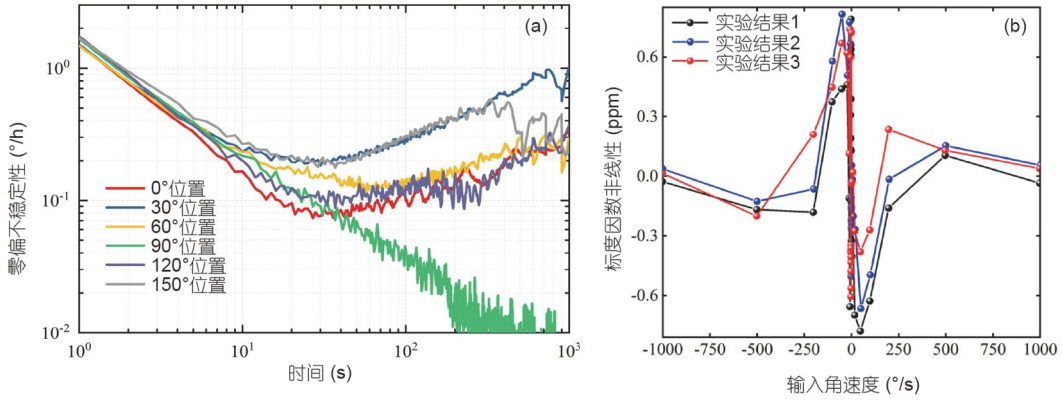


图 15　微半球谐振陀螺速率积分模式测试结果. (a) 零偏不稳定性测试; (b) 标度因数非线性测试[78]

Figure 15　Test results of rate integrated mode for themicro-hemispherical resonant gyroscope. (a) Test of bias instability; (b) test of scale factor nonlinearity [78].

误差[78]，验证了速率积分微半球谐振陀螺在高速旋转下的优异性能.

速率积分微机电的零偏误差主要来源于谐振结构阻尼不对称，导致零偏随着振型角度呈现周期性改变. 2022年美国加州大学欧文分校提出了一种基于振型自进动的零偏漂移误差抑制技术，通过施加静电力控制陀螺振型角旋转，达到平均谐振结构阻尼不对称的目的[127,128]. 同年日本东芝公司也提出了类似方案，将振型进动速度设定为135°/s，零偏不稳定性达到了0.1°/h，可以对地球自转角速度进行精确测量[129]. 南京理工大学将模态匹配技术与振型自进动技术结合，使陀螺在−30°C~60°C的温度范围内，零偏变化了1°，相比于传统速率积分工作模式降低了6倍以上[126].

4.3　频率调制模式

频率输出式微机电陀螺的探索最早追溯到2002年加州大学伯克利分校Seshia等人[130]研究的音叉共振式的微机电陀螺. 工作时陀螺中心的质量块处于谐振状态，当有角速度输入时，哥氏力使左右两个音叉周期性受拉压力发生刚度变化，并使得两个音叉的谐振频率朝相反方向变化，通过检测左右音叉的谐振频率差异从而解调出输入角速度. 2011年，加州大学Zotov等人发现微机电陀螺的谐振频率会随输入角速度的变化而改变，系统建立了频率输出式微机电陀螺的理论模型，并设计了四质量块频率输出式微机电陀螺，测量范围超过2000°/s[131~133]. 此外，他们还研究了模态驱动力在不同相位差时的频率输出[134]，为正交式频率输出陀螺和利萨如式频率输出陀螺研究奠定了基础.

2018年，我国北京计算科学研究中心基于量子力学方法推导了频率输出式微机电陀螺的理论模型[135]. 国防科技大学基于盘形微机电陀螺测试了正交式频率输出陀螺的标度因数及其温度稳定性, 测试结果如图16

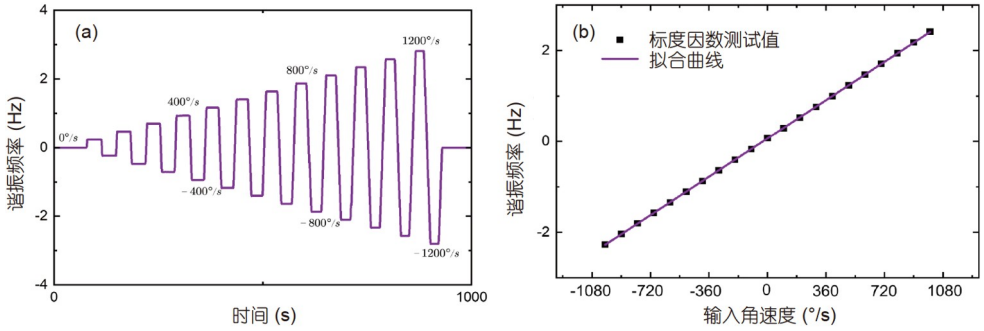


图 16　频率调制模式标度因数稳定性测试结果. (a) 测量范围测试; (b) 标度因数测试[136]

Figure 16　Test results of scale factor stability for frequency modulation mode. (a) Test of measurement range; (b) test of scale factor [136].

所示. 陀螺在常温20°C下的标度因数为0.00234 Hz/(°/s), 且在–20°C~80°C范围内标度因数稳定性优于17 ppm/°C. 双正交频率差分模式将零偏不稳定性提高至1.5°/h~6°/h, 体现出良好的长期稳定性与重复性.

5 高精度微机电陀螺发展趋势

5.1 集成化趋势

将微加速度计、微机电陀螺、微型原子钟等器件进行深度融合, 形成尺寸仅为立方厘米甚至毫米的高度集成的微型化惯性测量单元(IMU), 构建不依赖于卫星导航系统的芯片级微PNT系统, 适用于拒止环境下定位导航服务, 具有广阔的应用前景[137], 也是构成未来国家PNT体系的重要组成部分.

同时, 通过各器件之间深度融合, 以提升单个器件性能的相关研究也受到关注[138]. 如应用于微机电陀螺的时钟锁频技术, 利用高精度时钟基准为陀螺和加速度计提供参考, 使陀螺的谐振频率与原子钟的频率基准同步锁定, 有效提升陀螺频率稳定性, 可以将谐振陀螺的精度提高数个数量级. 例如美国Boeing公司、休斯研究所(HRL)等单位利用石英晶振在微机电陀螺中实现了频率锁定, 陀螺频率漂移可控制在2 ppb以内[137,139]. 为未来微惯性测量单元实现内部多源异质集成、跨尺度多物理场耦合奠定了基础.

5.2 面向极端条件应用发展趋势

弹药等武器装备是微机电陀螺应用最为广泛的领域之一, 随着装备机动性和精度不断提升, 日益要求其惯性器件在强冲击、高动态等极端条件下也具备良好的性能. 制导炮弹发射时, 冲击加速度峰值超过20000 g, 而新型电磁炮等武器弹药更是要承受超高的瞬间冲击力. 加州大学伯克利分校、Honeywell公司、英国航天航空公司(BAE)、法国THALES公司、我国中北大学、南京理工大学、国防科技大学等单位对此开展了长期研究[140,141], 但总体而言极端工况下微机电陀螺产生的零偏稳定性、标度因数等性能退化现象较为严重. 此外, 20 rad/s以上高转速下角度、角速度测量等问题也亟待解决. 因此开展微机电陀螺的创新研究, 突破结构简单、能够适应大过载、大量程的微机电陀螺相关技术, 对提升武器装备的打击精度、打击距离等指标具有重要的意义.

5.3 智能化发展趋势

随着微系统集成化能力的提升, 微机电陀螺与嵌入式系统芯片(MCU)融合, 不但具有信息采集功能, 还具有信息处理和交互能力, 从而实现智能化, 也是未来的重要发展方向之一. 信息处理能力的增强使模态操控、模态调制等新控制技术得以运用, 对误差漂移能做出更好预测, 使部分微机电陀螺初步具备了自补偿、自校准等功能, 精度得到进一步提升. 此外, 深度学习、神经网络等信息处理方法应用, 也使微机电陀螺能够具有更好的环境适应性[142,143].

6 结论与讨论

高精度的微机电陀螺是惯性领域的热点研究方向之一, 本文重点梳理了高精度微机电陀螺的结构演变规律、品质提升方法, 以及前沿控制技术的研究现状, 并对该领域发展趋势进行了展望, 为未来相关研究工作提供一些启示. 论文总结如下.

(1) 在高精度微机电陀螺谐振结构演变上, 双质量块、四质量块、环形微机电陀螺以及微半球谐振陀螺均有较好的性能报道, 部分产品已优于战术级精度指标, 少数已接近导航级精度门槛. 随着拓扑优化设计、新材料、新工艺的应用, 微机电陀螺的结构创新仍然值得期待.

(2) 微机电陀螺谐振结构的品质因数调控方法、质量平衡方法等研究有效促进了结构优化设计与品质提升, 为高精度微机电陀螺性能进一步提升提供了新的方法手段.

(3) 随着微机电陀螺表头性能提升, 速率积分等先进控制模式使其在高旋等应用场景发挥出独特的优势, 有望取得更加广泛的应用. 模态交换、非线性控制等新技术为陀螺性能提升提供了新思路.

(4) 对高性能微机电陀螺的发展趋势进行了展望, 一是高度集成化的芯片级微PNT系统已初现端倪; 二是满足大过载、大量程等极端条件应用的高性能微机电陀螺将具有广阔的空间; 三是随着微系统集成能力、信息处理能力的提升, 微机电陀螺的智能化水平也有望在未来不断增强.

参考文献

1 Derek K S. MEMS inertial sensors: A tutorial overview. IEEE Commun Mag, 2013, 51: 100−109

2 Ian B F, Chae H A, Eldwin J N, et al. Stochastic method for disk resonating gyroscope mode matching and quadrature nulling. In: Proceedings of IEEE International Conference on MICRO Electro Mechanical Systems. Shanghai, 2016. 998−1001

3 Zhu W, Wallace C S, Yazdi N. A tri-fold inertial measurement unit fabricated with a batch 3D assembly process. In: Proceedings of IEEE International Symposium on Inertial Sensors and Systems. Laguna Beach, 2016. 70−73

4 Cho J Y, Woo J K, Yan J, et al. Fused-silica micro birdbath resonator gyroscope (μ-BRG). J Microelectromech Syst, 2014, 23: 66–77

5 Zega V, Minotti P, Mussi G, et al. The first frequency-modulated (FM) pitch gyroscope. Proceedings, 2017, 1: 393

6 Minotti P, Dellea S, Mussi G, et al. High scale-factor stability frequency-modulated MEMS gyroscope: 3-Axis sensor and integrated electronics design. IEEE Trans Ind Electron, 2018, 65: 5040–5050

7 Bordiga E, Bestetti M, Langfelder G. AGC-less operation of high-stability lissajous frequency-modulated MEMS gyroscopes. In: Proceedings of 20th International Conference on Solid-State Sensors, Actuators and Microsystems & Eurosensors. Berlin, 2019. 594−597

8 Saukoski M, Aaltonen L, Salo T, et al. Interface and control electronics for a bulk micromachined capacitive gyroscope. Sens Actuat A Phys, 2008, 147: 183–193

9 Saukoski M, Aaltonen L, Halonen K, et al. Integrated readout and control electronics for a microelectromechanical angular velocity sensor. In: Proceedings of European Solid-State Circuits Conference. Montreaux, 2006. 243−246

10 Alper S E, Akin T. A single-crystal silicon symmetrical and decoupled gyroscope on insulating substrate. In: Proceedings of 12th International Conference on Solid-State Sensors, Actuators and Microsystems (TRANSDUCERS). Boston, 2003. 1399−1402

11 Leoncini M, Bestetti M, Bonfanti A, et al. Fully integrated, 406 μA, 5°/hr full digital output lissajous frequency-modulated gyroscope. IEEE Trans Ind Electron, 2019, 66: 7386–7396

12 Weinberg M S, Kourepenis A. Error sources in in-plane silicon tuning-fork MEMS gyroscopes. J Microelectromech Syst, 2006, 15: 479–491

13 Zaman M F, Sharma A, Zhili Hao A, et al. A mode-matched silicon-yaw tuning-fork gyroscope with subdegree-per-hour allan deviation bias instability. J Microelectromech Syst, 2008, 17: 1526–1536

14 Trusov A A, Prikhodko I P, Zotov S A, et al. Low-dissipation silicon tuning fork gyroscopes for rate and whole angle measurements. IEEE Sens J, 2011, 11: 2763–2770

15 Dellea S, Rey P, Langfelder G. MEMS gyroscopes based on piezoresistive NEMS detection of drive and sense motion. J Microelectromech Syst, 2017, 26: 1389–1399

16 Gadola M, Buffoli A, Sansa M, et al. 1.3 mm^2 Nav-grade NEMS-based gyroscope. J Microelectromech Syst, 2021, 30: 513–520

17 Sharma A, Zaman F M, Amini B V, et al. A high-Q in-plane SOI tuning fork gyroscope. In: Proceedings of IEEE Sensors Conference. Vienna, 2004. 467–470

18 Lapadatu D, Blixhavn B, Holm R, et al. SAR500–A high-precision high-stability butterfly gyroscope with north seeking capability. In: Proceedings of Position Location and Navigation Symposium. Indian Wells, 2010. 6−13

19 Hou Z, Kuang Y, Ou F, et al. A quadrature compensation method to improve the performance of the butterfly vibratory gyroscope. Sens Actuat A Phys, 2021, 319: 112527

20 Walther A, Savoye M, Jourdan G, et al. 3-Axis gyroscope with Si nanogage piezo-resistive detection. In: Proceedings of IEEE International Conference on Micro Electro Mechanical Systems. Paris, 2012. 480−483

21 Walther A, Desloges B, Lejuste C, et al. Development of a 3D capacitive gyroscope with reduced parasitic capacitance. J Micromech Microeng, 2013, 23: 025013

22 Burgess J, Curt A, Todd B, et al. Development of a navigation-grade MEMS IMU. In: Proceedings of IEEE International Symposium on Inertial Sensors and Systems. Kona, 2021. 1−4

23 Xia D, Chen S, Wang S, et al. Microgyroscope temperature effects and compensation-control methods. Sensors, 2009, 9: 8349–8376

24 Jiang J P. On-chip temperature control and compensation for silicon micro-gyroscope (in Chinese). Dissertation for the Master's Degree. Nanjing: Southeast University, 2012 [江金平. 基于片内热元件的硅微陀螺仪温度控制与补偿技术研究. 硕士学位论文. 南京: 东南大学, 2012]

25 Xia D Z, Wang S R, Zhou B L. ZRO temperature dependency compensating-control design of micro-gyro (in Chinese) . J Southeast Univ (Nat Sci Edi), 2012, 42: 290–294 [夏敦柱, 王寿荣, 周百令. 硅微陀螺仪零偏温度性能补控方法设计. 东南大学学报: 自然科学版, 2012, 42: 290–294]

26 Cao H L, Li H S, Wang S R, et al. Temperature compensation of monitoring circuit for silicon MEMS gyroscope (in Chinese). Opt Precision Eng, 2013, 21: 3118–3125 [曹慧亮, 李宏生, 王寿荣, 等. 硅微机械陀螺仪测控电路的温度补偿. 光学精密工程, 2013, 21: 3118−3125]

27 Shi Q, Qiu A P, Su Y. Study on the effects of machining error on the Z-axis silicon microgyroscope (in Chinese). Chin J Sensors Actuators, 2006, 19: 2182−2185 [施芹, 裘安萍, 苏岩. 硅微陀螺仪的误差分析. 传感技术学报, 2006, 19: 2182−2185]

28 Shi Q, Qiu A P, Su Y. Mechanical coupling error of silicon microgyroscope (in Chinese). Opt Precision Eng, 2008, 16: 894–898 [施芹, 裘安萍, 苏岩. 硅微陀螺仪的机械耦合误差分析. 光学精密工程, 2008, 16: 894–898]

29 Wang Y C, Wang Y, Meng B, et al. The development of a high accuracy tuning fork vibratory MEMS gyroscope (in Chinese). In: Proceedings of the China Aerospace Science and Technology Conference. Shenyang, 2019. 18–24 [王玉朝, 王永, 孟冰, 等. 高精度音叉式硅微陀螺研制进展. 见: 中国航空科学技术大会论文集. 沈阳, 2019. 18–24]

30 Kwok P Y, Weinberg M S, Breuer K S. Fluid effects in vibrating micromachined structures. J Microelectromech Syst, 2005, 14: 770–781

31 Sharma A, Zaman M F, Ayazi F. A sub-0.2°/hr bias drift micromechanical silicon gyroscope with automatic CMOS mode-matching. IEEE J Solid State Circuits, 2009, 44: 1593–1608

32 Asadian M H, Askari S, Shkel A M. An ultrahigh vacuum packaging process demonstrating over 2 million Q-factor in MEMS vibratory gyroscopes. IEEE Sens Lett, 2017, 1: 1–4

33 Trusov A, Rozelle D, Atikyan G, et al. Non-axisymmetric coriolis vibratory gyroscope with whole angle, force rebalance, and self-calibration. In: Proceedings of Solid-State Sensors, Actuators and Microsystems Workshop. Hilton Head Island, 2014. 419–422

34 Askari S, Asadian M, Kakavand K, et al. Near-navigation grade quad mass gyroscope with Q-factor limited by thermo-elastic damping. In: Proceedings of Solid-State Sensors, Actuators and Microsystems Workshop. Hilton Head Island, 2016. 254–257

35 Song M, Zhou B, Zhang T, et al. Parametric drive of a micro rate integrating gyroscope using discrete electrodes. In: Proceedings of IEEE International Symposium on Inertial Sensors and Systems. Kauai, 2017. 70–73

36 Zhang T, Zhou B, Song M, et al. Structural parameter identification of the center support quadruple mass gyro. IEEE Sens J, 2017, 17: 3765–3775

37 Zhang T, Zhou B, Yin P, et al. Optimal design of a center support quadruple mass gyroscope (CSQMG). Sensors, 2016, 16: 613

38 Hedenstierna N, Habibi S, Nilsen S. Bulk micromachined angular rate sensor based on the ‘butterfly’ gyro structure. In: Proceedings of IEEE International Conference on Micro Electro Mechanical Systems. Interlaken, 2001. 178−183

39 Safran. STIM300 Datasheet. 2022, https://www.sensonor.com/products/inertial-measurement-units/stim300/

40 Hou Z Q. Study on key technologies of improvement in bias stability of the micromachined butterfly gyroscope (in Chinese). Dissertation for the Doctoral Degree. Changsha: National University of Defense Technology, 2012 [侯占强. 蝶翼式微陀螺零偏不稳定性提升关键技术研究. 博士学位论文. 长沙: 国防科技大学, 2012]

41 Hou Z, Xiao D, Wu X, et al. Effect of axial force on the performance of micromachined vibratory rate gyroscopes. Sensors, 2010, 11: 296–309

42 Hou Z, Xiao D, Wu X, et al. Effect of die attachment on key dynamical parameters of micromachined gyroscopes. Microsyst Technol, 2012, 18: 507–513

43 Hou Z, Wu X, Xiao D, et al. Transition interface for improving the temperature characteristics of micromachined gyroscopes. Microsyst Technol, 2014, 20: 227–234

44 Cao S, Chen Z H, Xiao D B, et al. Analysis of improving ‘butterfly’ gyroscope’s sensitivity with a hexagon oblique beam. In: Proceedings of International Conference of CSMNT. Chengdu, 2014. 9−13

45 Wang X H, Xiao D B, Wu X Z, et al. Out-of-plane micro-force function generator based on polymeric thermal actuators for modifying micro-deformation. Appl Phy Lett, 2014, 20: 227–234

46 Su J, Xiao D, Wang X, et al. Vibration sensitivity analysis of the ‘butterfly-gyro’ structure. Microsyst Technol, 2014, 20: 1281–1290

47 Li W, Xiao D, Wu X, et al. Enhanced temperature stability of sensitivity for MEMS gyroscope based on frequency mismatch control. Microsyst Technol, 2017, 23: 3311–3317

48 Putty M W, Najafi K. A micromachined vibrating ring gyroscope. In: Proceedings of Solid-State Sensors and Actuators Workshop. Hilton Head Island, 1994. 213−220

49 Ayazi F, Najafi K. A HARPSS polysilicon vibrating ring gyroscope. J Microelectromech Syst, 2001, 10: 169–179

50 He G H, Najafi K. A single-crystal silicon vibrating ring gyroscope. In: Proceedings of IEEE International Conference on Micro Electro Mechanical Systems. Vegas, 2002. 718−721

51 Yazdi N, Ayazi F, Najafi K. Micromachined inertial sensors. Proc IEEE, 1998, 86: 1640–1659

52 Silicon Sensing. CRH02 Technical Datasheet. 2016, https://www.siliconsensing.com

53 Challoner A D, Ge H H, Liu J Y. Boeing disc resonator gyroscope. In: Proceedings of IEEE ION Position, Location and Navigation Symposium. Monterey, 2014. 504−514

54 Prikhodko I P, Gregory J A, Clark W A, et al. Mode-matched MEMS coriolis vibratory gyroscopes: Myth or reality. In: Proceedings of IEEE ION Position, Location and Navigation Symposium. Savannah, 2016. 1−4

55 Prikhodko I P, Nadig S, Gregory J A, et al. Half-a-month stable 0.2 degree-per-hour mode-matched MEMS gyroscope. In: Proceedings of IEEE International Symposium on Inertial Sensors and Systems. Kauai, 2017. 1−4

56 Ge H H, Liu J Y, Buchanan B. Bias self-calibration techniques using silicon disc resonator gyroscope. In: Proceedings of IEEE International Symposium on Inertial Sensors and Systems. Hapuna Beach, 2015. 1−4

57 Sorenson L, Ayazi F. Effect of structural anisotropy on anchor loss mismatch and predicted case drift in future micro-hemispherical resonator gyros. In: Proceedings of IEEE ION Position, Location and Navigation Symposium. Monterey, 2014. 493−498

58 Wang Y, Asadian M H, Shkel A M. Frequency split reduction by directional lapping of fused quartz micro wineglass resonators. In: Proceedings of IEEE International Symposium on Inertial Sensors and Systems. Kauai, 2017. 78−81

59 Senkal D, Ahamed M J, Ardakani M H A, et al. Demonstration of 1 million Q-factor on microglassblown wineglass resonators with out-of-plane electrostatic transduction. J Microelectromech Syst, 2015, 24: 29–37

60 Heidari A, Chan M L, Yang H A, et al. Micromachined polycrystalline diamond hemispherical shell resonators. In: Proceedings of International Conference on Solid-State Sensors, Actuators and Microsystems. Barcelona, 2013. 2415−2418

61 Cho J, Singh S, Nagourney T, et al. High-Q navigation-grade fused-silica micro birdbath resonator gyroscope. In: Proceedings of IEEE Sensors Conference. Sydney, 2021. 1−4

62 Shao P, Mayberry C L, Gao X, et al. A polysilicon microhemispherical resonating gyroscope. J Microelectromech Syst, 2014, 23: 762–764

63 Shao P, Tavassoli V, Liu C, et al. Electrical characterization of ALD-coated silicon dioxide micro-hemispherical shell resonators. In: Proceedings of IEEE International Conference on Micro Electro Mechanical Systems. Francisco, 2014. 612−615

64 Shao P, Tavassoli V, Mayberry C L, et al. A 3D-HARPSS polysilicon microhemispherical shell resonating gyroscope: Design, fabrication, and characterization. IEEE Sens J, 2015, 15: 4974–4985

65 Sorenson L D, Gao X, Ayazi F. 3-D micromachined hemispherical shell resonators with integrated capacitive transducers. In: Proceedings of IEEE International Conference on Micro Electro Mechanical Systems. Paris, 2012. 168−171

66 Bernstein J, Bancu M, Cook E, et al. Diamond hemispherical resonator fabrication by isotropic glass etch. In: Proceedings of Solid-State Sensors, Actuators and Microsystems Workshop. Hilton Head Island, 2014. 273−276

67 Bernstein J J, Bancu M G, Bauer J M, et al. High Q diamond hemispherical resonators: Fabrication and energy loss mechanisms. J Micromech Microeng, 2015, 25: 085006

68 Cho J Y, Singh S, Woo J K, et al. 0.00016 deg/hr angle random walk (ARW) and 0.0014 deg/hr bias instability (BI) from a 5.2M Q and 1-cm precision shell. In: Proceedings of IEEE International Symposium on Inertial Sensors and Systems. Hiroshima, 2020. 1−4

69 Luo B, Shang J, Zhang Y. Hemispherical glass shell resonators fabricated using chemical foaming process. In: Proceedings of IEEE Electronic Components and Technology Conference. San Diego, 2015. 2217−2221

70 Luo B, Shang J, Su Z, et al. Height adjustment of 3-D axisymmetric microumbrella shells for tailoring wineglass frequency. IEEE Trans Compon Packag Manufact Technol, 2018, 9: 567–574

71 Ruan Z, Ding X, Qin Z, et al. Modeling and compensation of assembly inclination error of micro hemispherical resonator gyroscope under force-to-rebalance mode. IEEE Sens J, 2021, 21: 14726–14738

72 Xu L, Luo B, Shang J, et al. Study on the effect of assembly errors on the electrostatic tuning ability in micro umbrella shell resonators. In: Proceedings of International Conference on Electronic Packaging Technology. Xiamen, 2021. 1−5

73 Fan Q, Lin C, Liu M, et al. High performance MEMS disk gyroscope with force-to-rebalance operation mode. In: Proceedings of IEEE Sensors Conference. New Delhi, 2018. 1−3

74 Ou F L. The optimal design of the wafer-level vacuum package butterfly vibratory gyroscope (in Chinese). Dissertation for the Doctoral Degree. Changsha: National University of Defense Technology, 2019 [欧芬兰. 圆片级真空封装蝶翼式微陀螺优化设计. 博士学位论文. 长沙: 国防科技大学, 2019]

75 Silicon Sensing. CRH03 Technical Datasheet. 2021, https://www.siliconsensing.com

76 Kim D, M'closkey R. A MEMS vibratory gyro with mode-matching achieved by resonator mass loading. In: Proceedings of IEEE/ION Position, Location and Navigation Symposium-PLANS. Monterey, 2014. 499–503

77 Xu Y, Li Q, Wang P, et al. 0.015 degree-per-hour honeycomb disk resonator gyroscope. IEEE Sens J, 2020, 21: 7326–7338

78 Sun J, Yu S, Zhang Y, et al. 0.79 ppm scale-factor nonlinearity whole-angle microshell gyroscope realized by real-time calibration of capacitive displacement detection. J Microsyst Nanoeng, 2021, 7: 79

79 Gerrard D D, Ahn C H, Flader I B, et al. Q–factor optimization in disk resonator gyroscopes via geometric parameterization. In: Proceedings of IEEE International Conference on Micro Electro Mechanical Systems. Shanghai, 2016. 994–997

80 Gerrard D D, Rodriguez J, Ortiz L C, et al. Manipulation of heat flux paths in thermo-elastically damped resonators for Q optimization. In: Proceedings of IEEE International Conference on Micro Electro Mechanical Systems. Vegas, 2017. 1130–1133

81 Xiao D, Zhou X, Li Q, et al. Design of a disk resonator gyroscope with high mechanical sensitivity by optimizing the ring thickness distribution. J Microelectromech Syst, 2016, 25: 606–616

82 Li Q S, Xiao D B, Zhou X, et al. 0.04 degree-per-hour MEMS disk resonator gyroscope with high-quality factor (510 k) and long decaying time constant (74.9 s). J Microsyst Nanoeng, 2018, 4: 32

83 Li Q S, Xiao D B, Xu Y, et al. Nonlinearity reduction in disk resonator gyroscopes based on the vibration amplification effect. IEEE Trans Ind Electron, 2019, 67: 6946–6954

84 Darvishian A, Shiari B, Cho J Y, et al. Anchor loss in hemispherical shell resonators. J Microelectromech Syst, 2017, 26: 51–66

85 Nitzan S H, Zega V, Li M, et al. Self-induced parametric amplification arising from nonlinear elastic coupling in a micromechanical resonating disk gyroscope. Sci Rep, 2015, 5: 9036

86 Ahn C H, Ng E J, Hong V A, et al. Geometric compensation of (100) single crystal silicon disk resonating gyroscope for mode-matching. In: Proceedings of International Conference on Solid-State Sensors, Actuators and Microsystems. Barcelona, 2013. 1723–1726

87 Ahn C H, Ng E J, Hong V A, et al. Mode-matching of wineglass mode disk resonator gyroscope in (100) single crystal silicon. J Microelectromech Syst, 2015, 24: 343–350

88 Fan B, Guo S, Yu L, et al. A novel sixteen-sided cobweb-like disk resonator gyroscope with low as-fabricated frequency split between drive and sense modes. In: Proceedings of IEEE Sensors Conference. New Delhi, 2018. 1–4

89 Xiao D, Yu D, Zhou X, et al. Frequency tuning of a disk resonator gyroscope via stiffness perturbation. IEEE Sens J, 2017, 17: 4725–4734

90 Marjoux D, Ullah P, Frantz R N, et al. Silicon MEMS by Safran-navigation grade accelerometer ready for mass production. In: Proceedings of IEEE DGON Inertial Sensors and Systems. Braunschweig, 2020. 1–18

91 Emerard J D, Auger J, Mace J S, et al. Si-MEMS gyro by Safran: Towards the navigation grade. In: Proceedings of IEEE International Symposium on Inertial Sensors and Systems. Kailua Kona, 2022. 1–4

92 Schwartz D, Kim D, M'closkey R. A model-based approach to multi-modal mass tuning of a micro-scale resonator. In: Proceedings of American Control Conference. Montreal, 2012. 98–103

93 Kim D, Closkey R M. A MEMS vibratory gyro with mode-matching achieved by resonator mass loading. In: Proceedings of IEEE ION Position, Location and Navigation Symposium. Montreal, 2014. 499–503

94 Viswanath A, Li T, Gianchandani Y. High resolution micro ultrasonic machining for trimming 3D microstructures. J Micromech Microeng, 2014, 24: 065017

95 Hamelin B, Tavassoli V, Ayazi F. Localized eutectic trimming of polysilicon microhemispherical resonating gyroscopes. IEEE Sens J, 2014, 14: 3498–3505

96 Li B, Xi X, Lu K, et al. Study of electrode ablation for femtosecond laser trimming of micro hemispherical resonator gyroscope. IEEE Sens J, 2023, 23: 1933–1942

97 Shcheglov K, Evans C, Gutierrez R, et al. Temperature dependent characteristics of the JPL silicon MEMS gyroscope. In: Proceedings of IEEE Aerospace Conference. Big Sky, 2000. 403–411

98 Keymeulen D, Peay C, Yee K, et al. Effect of temperature on MEMS vibratory rate gyroscope. In: Proceedings of IEEE Aerospace Conference.

Big Sky, 2005. 1−6
99 Wong C L, Palaniapan M. Phonon detection technique for the study of the temperature coefficient of resonance frequency in clamped–clamped beam resonators. J Micromech Microeng, 2009, 19: 065021
100 Zhang X, Park S, Judy M W. Accurate assessment of packaging stress effects on MEMS sensors by measurement and sensor–package interaction simulations. J Microelectromech Syst, 2007, 16: 639–649
101 Zhang X, Park S, Navarro R, et al. Accurate assessment of packaging stress effects on MEMS devices. In: Proceedings of Intersociety Conference on ITHERM. San Diego, 2006. 1336−1342
102 Joo J W, Choa S H. Deformation behavior of MEMS gyroscope sensor package subjected to temperature change. IEEE Trans Comp Packag Technol, 2007, 30: 346–354
103 Maeda D, Ono K, Giner J. MEMS gyroscope with less than 1-deg/h bias instability variation in temperature range from −40°C to 125°C. Sensors, 2018, 18: 1006−1015
104 Fell C P. Development of a second generation low cost MEMS gyroscope: Design for manufacture. In: Proceedings of Seminar on MEMS Sensors & Actuators. London, 2006. 75−82
105 Sturland I. Development and commercialisation of silicon MEMS gyroscopes. In: Proceedings of IEEE Seminar and Exhibition on MEMS Sensor Technologies. London, 2005. 1−3
106 Zaman M F, Sharma A, Ayazi F. The resonating star gyroscope: A novel multiple-shell silicon gyroscope with sub-5 deg/hr allan deviation bias instability. IEEE Sens J, 2009, 9: 616–624
107 Lee S H, Lee S W, Najafi K. A generic environment-resistant packaging technology for MEMS. In: Proceedings of Solid-State Sensors, Actuators and Microsystems Conference. Lyon, 2007. 335−338
108 Lee S H, Cho J, Lee S W, et al. A low-power ovencontrolled vacuum package technology for high-performance MEMS. In: Proceedings of IEEE International Conference on Micro Electro Mechanical Systems. Sorrento, 2009. 753−756
109 Kim B, Hopcroft M A, Candler R N, et al. Temperature dependence of quality factor in MEMS resonators. J Microelectromech Syst, 2008, 17: 755–766
110 Salvia J C, Melamud R, Chandorkar S A, et al. Real-time temperature compensation of MEMS oscillators using an integrated micro-oven and a phase-locked loop. J Microelectromech Syst, 2010, 19: 192–201
111 Ahn C H, Hong V A, Park W, et al. On-chip ovenization of encapsulated disk resonator gyroscope (drg). In: Proceedings of Solid-State Sensors, Actuators and Microsystems. Anchorage, 2015. 39−42
112 He C H, Zhao Q C, Liu Y X, et al. Closed loop control design for the sense mode of micromachined vibratory gyroscopes. Sci China Tech Sci, 2013, 5: 1112−1118
113 Trusov A A, Phillips M R, Mccammon G H, et al. Continuously self-calibrating CVG system using hemispherical resonator gyroscopes. In: Proceedings of IEEE International Symposium on Inertial Sensors & Systems. Hapuna Beach, 2015. 1−4
114 Kaajakari V, Mattila T, Oja A, et al. Nonlinear limits for single-crystal silicon microresonators. J Microelectromech Syst, 2004, 13: 715–724
115 Nitzan S, Su T H, Ahn C H, et al. Impact of gyroscope operation above the critical bifurcation threshold on scale factor and bias instability. In: Proceedings of IEEE International Conference on Micro Electro Mechanical Systems. San Francisco, 2014. 749−752
116 Lynch D D. Vibratory gyro analysis by the method of averaging. In: Proceedings of 2nd St Petersburg Conference on Gyroscopic Technology and Navigation. Petersburg, 1995. 26−34
117 Prikhodko I P, Zotov S A, Trusov A A, et al. Foucault pendulum on a chip: Rate integrating silicon MEMS gyroscope. Sens Actuat A Phys, 2012, 177: 67–78
118 Trusov A A, Prikhodko I P, Zotov S A, et al. Ultra-high Q silicon gyroscopes with interchangeable rate and whole angle modes of operation. In: Proceedings of IEEE Sensors Conference. Waikoloa, 2010. 864−867
119 Prikhodko I P, Gregory J A, Bugrov D I, et al. Overcoming limitations of rate integrating gyroscopes by virtual rotation. In: Proceedings of IEEE International Symposium on Inertial Sensors and Systems. Laguna Beach, 2016. 5−8
120 Senkal D, Ng E, Hong V, et al. Parametric drive of a toroidal MEMS rate integrating gyroscope demonstrating <20 ppm scale factor stability. In: Proceedings of IEEE International Conference on Micro Electro Mechanical Systems. Estoril, 2015. 29−32
121 Cho J, Nagourney T, Darvishian A, et al. Ultra conformal high aspect-ratio small-gap capacitive electrode formation technology for 3D micro shell resonators. In: Proceedings of IEEE International Conference on Micro Electro Mechanical Systems. Las Vegas, 2017. 1169−1172

122 Boyd C, Woo J K, Cho J Y, et al. Effect of drive-axis displacement on MEMS birdbath resonator gyroscope performance. In: Proceedings of IEEE International Symposium on Inertial Sensors and Systems. Kauai, 2017. 1–2
123 Woo J K, Cho J Y, Boyd C, et al. Whole-angle-mode micromachined fused-silica birdbath resonator gyroscope (WA-BRG). In: Proceedings of IEEE International Conference on Micro Electro Mechanical Systems. Francisco, 2014. 20–23
124 Taheri T P, Izyumin O, Izyumin I, et al. Disk resonator gyroscope with whole-angle mode operation. In: Proceedings of IEEE International Symposium on Inertial Sensors and Systems. Hapuna Beach, 2015. 1–4
125 Taheri-Tehrani P, Challoner A D, Horsley D A. Micromechanical rate integrating gyroscope with angle-dependent bias compensation using a self-precession method. IEEE Sens J, 2018, 18: 3533–3543
126 Fan Q, Zhou Y, Liu M, et al. A MEMS rate-integrating gyroscope (RIG) with in-run automatic mode-matching. IEEE Sens J, 2022, 22: 2282–2291
127 Askari S, Asadian M H, Shkel A M. Retrospective correction of angular gain by virtual carouseling in MEMS gyroscopes. In: Proceedings of IEEE International Symposium on Inertial Sensors and Systems. Naples, 2019. 1–4
128 Vatanparvar D, Shkel A M. On correlation of anisoelasticity, angular gain, and temperature in whole-angle CVGs. IEEE Sens J, 2021, 22: 4175–4185
129 Miyazaki F, Gando R, Ono D, et al. A 0.1 deg/h module-level silicon MEMS rate integrating gyroscope using virtually rotated donut-mass structure and demonstration of the earth's rotation detection. In: Proceedings of IEEE International Conference on Solid-State Sensors, Actuators and Microsystems. Orlando, 2021. 402–405
130 Seshia A A, Howe R T, Montague S. An integrated microelectromechanical resonant output gyroscope. In: Proceedings of IEEE International Conference on Micro Electro Mechanical Systems. Las Vegas, 2002. 722–726
131 Zotov S A, Prikhodko I P, Trusov A A, et al. Frequency modulation based angular rate sensor. In: Proceedings of IEEE International Conference on Micro Electro Mechanical Systems. Cancun, 2011. 577–580
132 Zotov S A, Trusov A A, Shkel A M. Demonstration of a wide dynamic range angular rate sensor based on frequency modulation. In: Proceedings of IEEE Sensors Conference. Limerick, 2011. 149–152
133 Zotov S A, Trusov A A, Shkel A M. High-range angular rate sensor based on mechanical frequency modulation. J Microelectromech Syst, 2012, 21: 398–405
134 Zotov S A, Prikhodko I P, Simon B, et al. Optimization of orbital trajectory for frequency modulated gyroscope. In: Proceedings of International Symposium on Inertial Sensors and Systems. Laguna Beach, 2014. 1–2
135 Li K, Fu H, Li Y. Coriolis-force-induced coupling between two modes of a mechanical resonator for detection of angular velocity. Phys Rev A, 2018, 98: 023862
136 Ren X J. Research on design method and control technology of quadrature frequency-modulated MEMS vibratory gyroscope (in Chinese). Dissertation for the Master's Degree. Changsha: National University of Defense Technology, 2021 [任幸晶. 正交式频率输出MEMS振动陀螺的设计方法与控制技术研究. 硕士学位论文. 长沙: 国防科技大学, 2021]
137 Kubena R L, Stratton F P, Huang L X, et al. Co-integration of a quartz Ocxo and Si MEMS inertial sensors for improved navigational accuracy. In: Proceedings of IEEE International Frequency Control Symposium. New Orleans, 2016. 1–6
138 Lutwak R. Micro-technology for positioning, navigation, and timing towards PNT everywhere and always. In: Proceedings of IEEE International Symposium on Inertial Sensors and Systems. Laguna Beach, 2014. 1–4
139 Kubena R L, Joyce R J, Challoner A D. Correlation of frequency, temperature, and bias stability of a Si ring gyro. In: Proceedings of IEEE International Symposium on Inertial Sensors and Systems. Laguna Beach, 2016. 21–24
140 Sheard K, Scaysbrook I, Cox D. MEMS sensor and integrated navigation technology for precision guidance. In: Proceedings of IEEE Position, Location & Navigation Symposium. Monterey, 2008. 1145–1151
141 Zhou X, Wu Y, Wu X, et al. A novel ring vibrating gyroscope based on side piezo-electrodes. J Cent South Univ, 2016, 23: 555–561
142 Guo W J, Cao H L. Temperature compensation of MEMS gyroscope based on variational mode decomposition and neural network algorithm (in Chinese). J Test Meas Technol, 2021, 35: 495–502 [郭文静, 曹慧亮. 基于变分模态分解和神经网络算法的微机械陀螺温度补偿. 测试技术学报, 2021, 35: 495–502]
143 Song Y P, Liu N, Liu F C, et al. Temperature error compensation method of MEMS gyroscope under deep learning (in Chinese). Chin J Sensors Actuators, 2022, 35: 92–98 [宋一平, 刘宁, 刘福朝, 等. 深度学习下MEMS陀螺温度误差补偿方法. 传感技术学报, 2022, 35: 92–98]

Research status and development trend of high-precision MEMS gyroscope

XI Xiang, SUN JiangKun, XIAO DingBang, ZHANG YongMeng, Li QingSong, ZHOU Xin, LU Kun, SHI Yan, HOU ZhanQiang & WU XueZhong

College of Intelligence Science and Technology, National University of Defense Technology, Changsha 410073, China

MEMS gyroscopes are widely used in industry and defense field equipment due to advantages such as small volume, light weight, and low cost. The use of a high-precision MEMS gyroscope can improve the accuracy of attitude measurement and provide control for a wide range of equipment and platforms, and it is expected to solve the problem of autonomous navigation in complex environments for unmanned vehicles, aerial vehicles, and other equipment. Owing to its appealing development prospects, the high-precision MEMS gyroscope remains one of the widely researched topics in the field of inertial technology. However, developing a high-precision MEMS gyroscope is challenging. First, this paper examines the evolution rules of the structure of a high-precision MEMS gyroscope, thus categorizing it as a mass block structure and spinning symmetric structure for performance analysis and comparison. Second, to improve the quality of the MEMS gyroscope resonator, this paper highlights the methods for improving the quality factor and adjusting the frequency of the microresonant structure and then introduces the research status of high-precision MEMS gyroscope control technology based on the rate mode, rate integrated mode, and frequency modulation mode. Finally, the future development and application trends of high-precision MEMS gyroscopes are anticipated.

high-precision MEMS gyroscope, resonant structure, bias instability, quality factor, frequency split, control technology

doi: 10.1360/SST-2023-0119